

Ultra Low-Cost Injection-locked FP Laser Source for Coherent Access Networks

A Technical Paper prepared for SCTE•ISBE by

Zhensheng(Steve) Jia, Ph.D.

Distinguished Technologist

CableLabs

858 Coal Creek Circle, Louisville CO, 80027

303.661.3364

s.jia@cablelabs.com

L. Alberto Campos, Ph.D.

Fellow

CableLabs

858 Coal Creek Circle, Louisville CO, 80027

303.661.3377

a.campos@cablelabs.com

Mu Xu, Ph.D., CableLabs

Haipeng Zhang, Ph.D., CableLabs

Junwen Zhang, Ph.D., CableLabs

Chris Stengrim, CableLabs

Curtis Knittle, Ph.D., CableLabs

Table of Contents

| Title | Page Number |
|-----------------------------------------------------------------------|--------------------|
| Table of Contents | 2 |
| Introduction | 3 |
| Content | 4 |
| 1. Coherent Optics for Access Networks | 4 |
| 2. Motivation of Injection-locked FP Source for Coherent Optics | 5 |
| 3. Operation Principle of FP Laser Injection Locking | 6 |
| 4. Design of Injection-locking Scheme | 7 |
| 5. Experimental Verifications | 14 |
| 6. Applications and Cost Analysis | 17 |
| Conclusions | 18 |
| Abbreviations | 18 |
| Bibliography & References | 19 |

List of Figures

| Title | Page Number |
|----------------------------------------------------------------------------------------------------------------------------------------------------------------------------------------------------------|--------------------|
| Figure 1 – Coherent Optics for Cable Access Applications | 4 |
| Figure 2 – FP laser cavity modes | 5 |
| Figure 3 – Optical injection locking setup: (a) transmission style; (b) reflection style | 7 |
| Figure 4 – Multi-beam interference model for an Fabry-Perot laser cavity | 8 |
| Figure 5 – Gain spectra of the Fabry-Perot cavity versus (a) reflectivity of the front facet, and (b) cavity length | 9 |
| Figure 6 – SMSR versus injection power at different wavelengths | 10 |
| Figure 7 – FP laser I-V curve (a) and output power vs. bias (b) | 10 |
| Figure 8 – Optical spectrum of the FP laser: (a) free running; (b) injection locked | 11 |
| Figure 9 – Injection locking process study: (a) locking map under different injection ratio and frequency detuning; (b) optical spectrums of the slave FP laser under different locking conditions | 13 |
| Figure 10 – Side mode suppression ratio under various frequency detuning | 13 |
| Figure 11 – Delayed self-heterodyne laser linewidth measurement setup | 14 |
| Figure 12 – Measured ECL and injection-locked FP-LD linewidth | 15 |
| Figure 13 – Measured low-cost DFB laser linewidth | 15 |
| Figure 14 – System diagram for BER measurement | 16 |
| Figure 15 – BER performance with and without applying COIL for (a) 32-Gbaud DP-QPSK, (b) 60.375-Gbaud DP-16QAM, and (c) 40-Gbaud DP-64QAM | 16 |
| Figure 16 – Application I: Multiple fibers to different destinations | 17 |
| Figure 17 – Application II: Comb source for DWDM systems over single fiber | 18 |

Introduction

The market for coherent optical links to reach between 10 km and 120 km is emerging in many application scenarios, such as router-to-router and point-to-point data center interconnect, mobile xhaul and cable aggregation applications. These market opportunities have catalyzed huge investment and development of new power and footprint optimized pluggable products in optical industry. In the cable environment, access networks have been undergoing significant technology and architecture changes driven by the ever-increasing residential data service tiers and an increasing number of services types being supported, such as business services and cellular connectivity. Digital fiber technologies and distributed access architecture (DAA) for fiber deep strategies offer an infrastructure foundation for cable operators to deliver the best service quality to the end users in the years ahead.

CableLabs® has recognized the need of coherent optics in the access network and has been working on point-to-point 100G and 200G coherent optics specifications. On June 29th, 2018, CableLabs publicly unveiled for the first time two new specifications: P2P Coherent Optics Architecture Specification and P2P Coherent Optics Physical Layer v1.0 Specification [1]. These two new specifications are the result of a focused effort by CableLabs, its members, and the manufacturer partners to develop Coherent Optics technology for the access network and to bring coherent optical technology to market quickly. On March 11, 2019, CableLabs announced another addition to its family of Point-to-Point Coherent Optics specifications: The P2P Coherent Optics Physical Layer v2.0 Specification [2]. This new specification defines interoperable P2P coherent optics links running at 200 Gbps (200G) on a single wavelength.

Low-cost coherent transceiver design is of great interest in bringing coherent optics to access networks because the existing commercially available coherent opto-electronic subsystems are associated with a high degree of complexity and cost for long haul and metro applications. Among different components of the coherent transceiver, active continuous-wave (CW) laser is of critical importance performing both transmitter source and receiver local oscillator (LO) for such low-cost coherent systems. The laser used in current coherent system is an external cavity laser, or ECL, which generates a narrower linewidth for coherent system needs. The typical linewidth of ECLs is ~50-500 kHz level. It uses a reflector that creates the cavity outside of the gain chip and allows the cavity to be longer than if it was confined to the gain chip alone. However, it is high cost and complicated, which is not attractive in access applications.

Fabry-Perot (FP) lasers, or FP laser diodes (FP-LD), on the other hand, is simple and ultra-low cost. Cable operators have deployed inexpensive FP lasers in the HFC upstream optical links for years. Unfortunately, FP lasers are not applicable for coherent optics in its current use. In this paper, we propose low-cost injection-locked FP laser source for coherent access applications. Through injection locking, the child laser closely adopts the optical frequency and linewidth characteristics of the parent laser which can be shared between multiple child lasers. As a result, the cost of the coherent optical transceiver can be significantly reduced. In this paper the injection locking technique is investigated by applying the external parent laser to multiple child FP-LDs. The static and dynamic characteristics are studied in detail, which include injection locking and detuning condition, linewidth reduction feature, output power maximization, and optimized design for coherent system. In addition, this paper discusses applications of injection locked FP-LDs and optical frequency combs in coherent access system and presents an experimental comparison of transmission performance with and without injection locking.

Content

1. Coherent Optics for Access Networks

Leveraging further development of CMOS processing, reduction in design complexity, and cost reduction of opto-electro components, coherent solutions are moving from long haul and metro to access networks. Access networks have been steadily evolving in their capabilities, architectures, and the type of services they carry. Cable has been deploying fiber deeper and migrating towards DAAs that bring fiber much closer to subscribers. These networks have a transition towards much greater capacity per subscriber, more fiber in closer proximity to subscribers, and the simultaneous delivery of all types of services. Coherent optics is a very suitable technology to address the long-term evolution of access networks.

Coherent optics for access networks enable superior receiver sensitivity that allows extended power budget and high frequency selectivity for closely spaced dense/ultra-dense WDM channels without the need of narrow-band optical filters. Moreover, the multi-dimensional signal recovered by coherent detection provides additional benefits to compensate linear transmission impairments such as chromatic dispersion (CD) and polarization mode dispersion (PMD), and efficiently utilizes the spectral resource, benefiting future network upgrades through the use of multi-level advanced modulation formats.

Coherent optics technology can be leveraged in cable following two general approaches. First is when used as a means of multi-link aggregation, and the second is through direct end-to-end connectivity to the desired end-point as shown in Figure 1. Following capacity growth trends, it is obvious that initially the aggregation use cases are going to outnumber the direct end-to-end connectivity use cases. The aggregation use case supports any DAA, including Remote PHY, Remote MAC-PHY, and Remote optical line terminal (OLT) architectures and cellular aggregations.

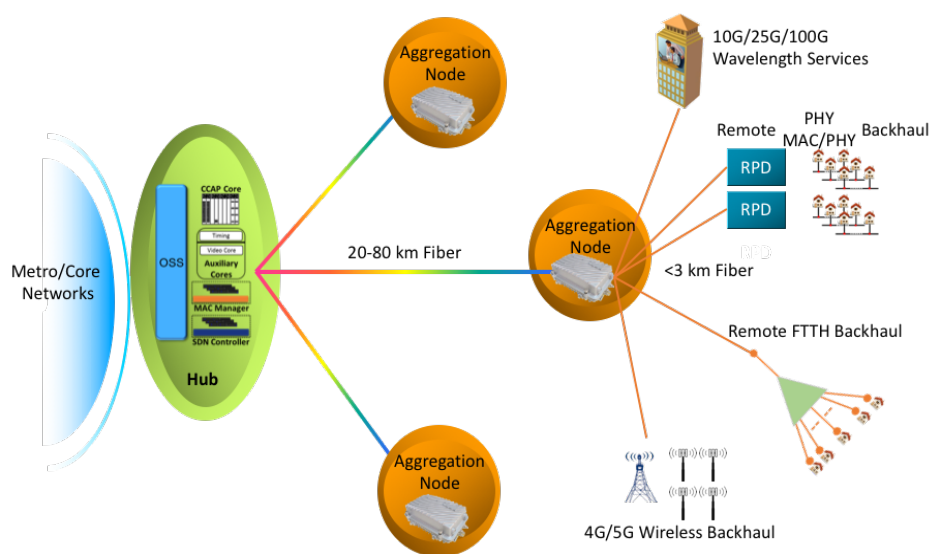


Figure 1 – Coherent Optics for Cable Access Applications

Aggregation would likely take place at the optical terminal where fiber has already been deployed and from where multiple new deeper fiber links are being extended. This is the location of the original HFC node, which is becoming this evolved optical node. In this aggregation use case, a device host called the Optical Distribution Center (ODC) or Aggregation Node terminates the downstream P2P coherent optic link that originated at the Headend or Hub, and outputs multiple optical or electrical Ethernet interfaces

operating at lower data rates to connect devices that are either colocated with the ODC and/or exist deeper in the network. This aggregation or disaggregation function can be done by a router, an Ethernet switch, or a Muxponder, depending on the DOCSIS®/PON/business traffic demand, cost, scalability/flexibility/reliability, and other operational considerations. The distance between the Hub and fiber nodes or future Aggregation Nodes ranges from 20 to 80 km, and the distance from the Aggregation Node to each end point is less than 3 km. Today the hubs typically support tens of nodes support multiple (~60) Aggregation Nodes for different services [3].

2. Motivation of Injection-locked FP Source for Coherent Optics

Cost reduction is the key to successfully bring coherent optics into high-volume access environments. Therefore, simplified coherent transceivers have been intensively researched in recent years. Laser source is one of the high-cost items in coherent transceiver structure. The laser used in current coherent system is an external cavity laser, or ECL, which generates a narrower linewidth for coherent system needs. The typical linewidth of ECLs is ~50-500kHz in range. It has a reflector that creates the cavity outside of the gain chip and allows the cavity to be longer than if it was confined to the gain chip. Having the external cavity in addition to the gain medium semiconductor structure imposes conditions that leads to single frequency and very fine linewidth emission. However, ECL implementation is high cost and complicated for access applications.

FP-LD, on the other hand, is simple and ultra-low-cost light sources for low data rate short distance optical communication. Cable operators have deployed inexpensive FP lasers in the HFC upstream optical links before. Figure 2 shows the basic operation principle of a multimode FP Laser, which has a basic structure of resonant cavity in a gain media, typically III-V group semiconductor. The resonance cavity is formed by having a front reflection mirror surface, and a rear reflection mirror surface. For optimized output power efficiency, the rear reflection mirror usually has a higher reflectivity than the front mirror surface. A stable resonant mode is formed by meeting the following two conditions. First, an integer number of wavelengths is equal to the round-trip optical path of the laser cavity. Second, the resonant mode is within the gain media spectral range. Mathematically, the laser modal wavelength λ relates to the laser resonance cavity length L by the equation $N\lambda=2L$. N is a positive integer larger than one. Despite their low cost, FP lasers are not applicable for coherent system in their current use due to limited performance in terms of multiple modes and linewidth of each mode.

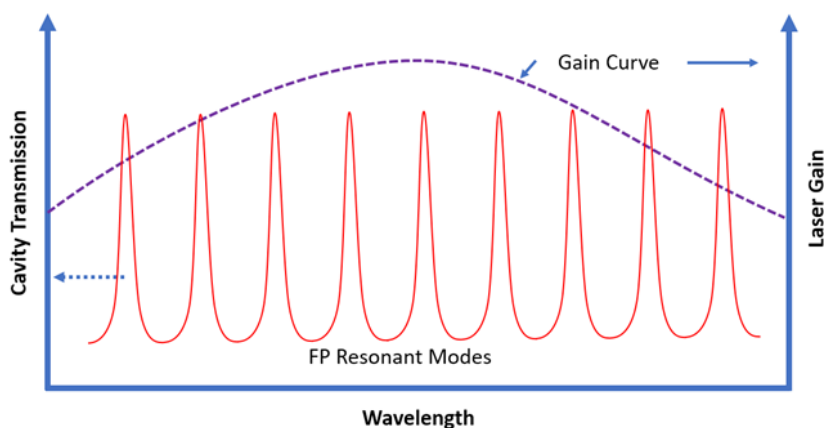


Figure 2 – FP laser cavity modes

In traditional operation of an FP laser, the wider linewidth that is typical for a FP laser structure would result in excessive phase noise and the inability to distinguish one constellation point from the other. In addition, FP-LD generation of multiple modes above the gain threshold and transmission of all these simultaneously modulated modes leads to excessive interference with no practical way to distinguish information.

The question we asked ourselves is if there is a way to predominantly excite and promote the generation and emission of a single mode of very narrow linewidth that can meet the signal criteria of coherent systems. Traditionally, this has been achieved by changes in the laser structure which has been the case in the more complex laser structures such as distributed feedback lasers and ECLs. This paper describes how a simple FP laser structure can be excited with an external optical signal to generate a high spectral purity source that suitable for use in coherent systems. A specific optical signal processing called optical injection locking can be used in generating this high spectral purity signal with an FP laser diode and enable low-cost FP lasers based coherent systems.

3. Operation Principle of FP Laser Injection Locking

Optical injection locking (OIL) refers to the phenomenon under which the laser subjected to the external injection (the so-called slave laser or child laser) is phase and frequency locked to the external signal originating from a free running laser (the so-called master laser or parent laser). Since a semiconductor laser can be locked to frequency and phase of an externally injected optical signal through the injection locking process, a low-cost multi-mode FP laser diode can be turned into single-mode operation by injecting a high-quality single-mode signal into its cavity. The injection locked laser systems can improve a host of fundamental limitations in simple FP lasers: single mode operation and side-mode suppression, enhanced modulation bandwidth, suppressed nonlinear distortion, reduced intensity noise and chirp, etc. [4-6]. Schematic setup of an optical injection locking system is shown in Figure 3 ((a): transmission style; (b): reflection style). In the transmission style system, the light from the master laser is injected into a slave FP laser. It's polarization is adjusted by a polarization controller (PC) to match the slave laser cavity mode. An optical isolator is placed between the master and the slave laser to prevent back reflection. The injected master light enters the slave FP laser cavity through one of its facets and the output light exits through the other facet. In the reflection style system, the injected master light and the output light utilize the same facet to enter or exit the FP laser cavity, a laser design feature commonly found in commercial products. The master laser injects light into the FP laser via a three-port optical circulator, and the output from the FP laser exits the same optical circulator. When wavelength of the light from the master laser is set within a certain frequency detuning range with respect to the slave laser, the slave laser's wavelength is pulled towards the master's, until the dynamics of the laser settle with its frequency and phase both locked to the master laser.

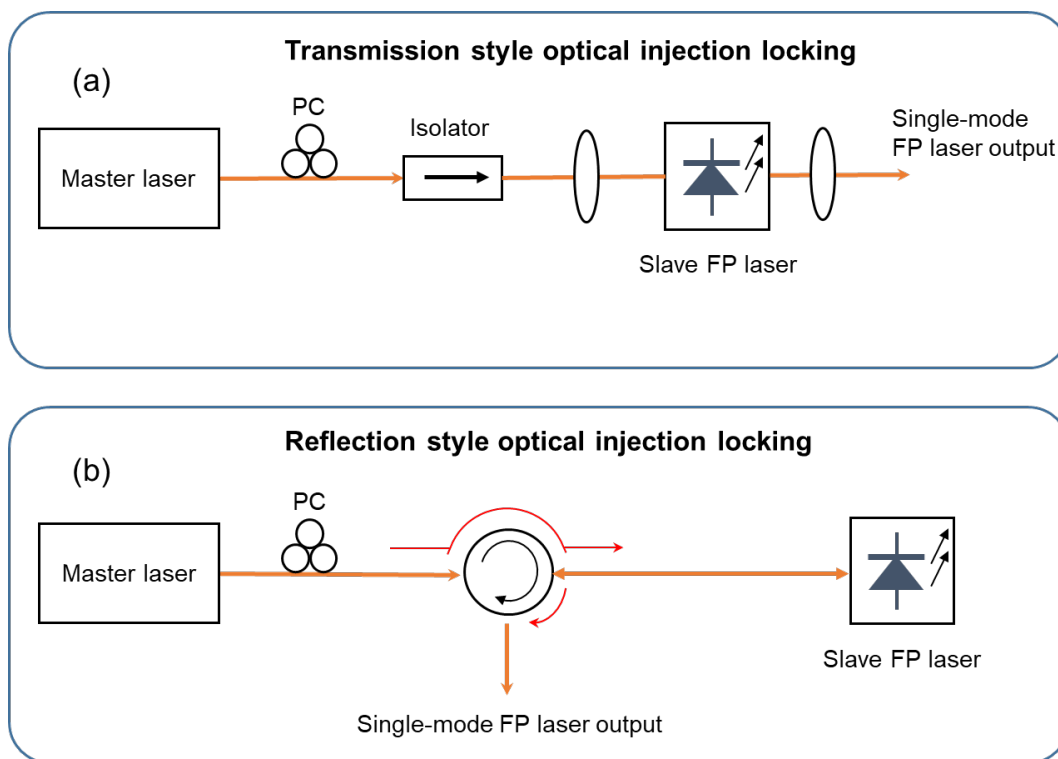


Figure 3 – Optical injection locking setup: (a) transmission style; (b) reflection style

4. Design of Injection-locking Scheme

The peak frequency is the master laser frequency which the FP laser under test locks. One important characteristic of injection locking of FP laser is that the locking frequency peak is much higher than the side modes of the FP laser. This parameter is called side mode suppression ratio (SMSR). As a rule of thumb, SMSR of 30 dB or higher is regarded as good optical injection locking. Higher SMSR will provide better transmission distance with reduced phase and amplitude noise. Practical SMSR needed depends on specific link budget requirement.

The Fabry-Perot cavity can be simplified as a mirror-gain medium-mirror (MGM) structure as shown in Figure 4, where the gain medium in the middle is isolated by two reflective mirrors from the air. These mirrors could be made of thin films or coatings, which are characterized by certain coefficients of transmissivity and reflectivity. When the light is projected onto the surface of the mirror, part of the light is reflected, and another part of the light penetrates through the mirror and injects into the gain medium. The injected light passing through the front mirror will be bounced multiple times inside the cavity. After each round trip in the cavity, there will be a small part of light leaked out through the front mirror. At a certain wavelength when all these lights can constructively add together, the output power will reach a maximum value. Such a wavelength is referred as an intrinsic longitudinal mode in FP-LD, where the light waves can form a stable standing wave inside the cavity. The wavelengths that fulfill the constructive interference condition will exhibit multiple peaks at the power transmission curve, which is the reason for the multi-mode nature in an FP-LD. In the following section, the multi-mode property of FP-LD and the related factors affecting the design of FP-LD are analyzed in detail.

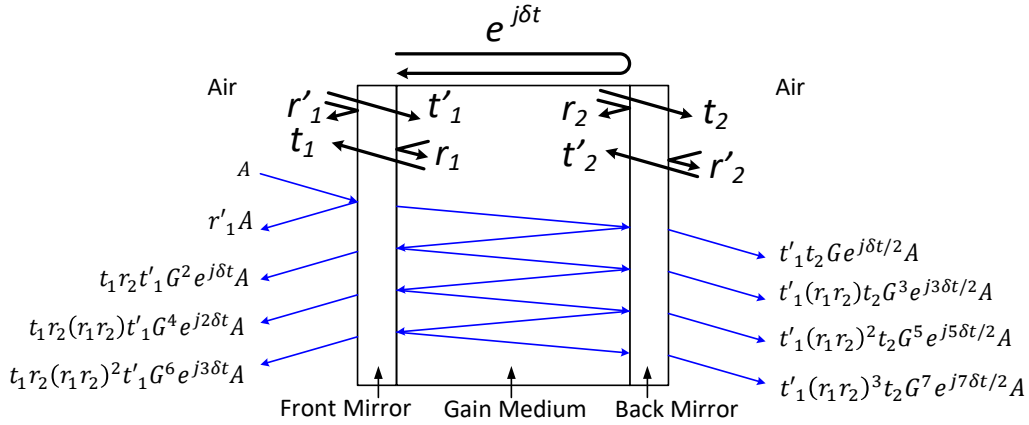


Figure 4 – Multi-beam interference model for an Fabry-Perot laser cavity

As shown in Figure 4, the transmission and reflection coefficients of the outer and inner layers for the front mirror are denoted as t_1 , t'_1 , r_1 , and r'_1 respectively. Similarly, the transmission and reflection coefficients of the inner and outer layers for the back mirror are t_2 , t'_2 , r_2 , and r'_2 respectively. Also, the gain and phase shift of one-round trip inside the cavity are provided as G and δ , respectively. When electrical field A is given as the input, the output lights after the initial three round-trips inside the cavity can be given as $r'_1 A$, $t_1 r_2 t'_1 G^2 e^{j\delta t} A$, and $t_1 r_2 (r_1 r_2) t'_1 G^4 e^{j2\delta t} A$. Adding these terms together, the output electric field of the light is

$$\begin{aligned} E_{out} &= r'_1 A + t_1 r_2 t'_1 G^2 e^{j\delta t} A + t_1 r_2 (r'_1 r_2) t'_1 G^4 e^{j2\delta t} A + t_1 r_2 (r'_1 r_2)^2 t'_1 G^6 e^{j3\delta t} A + \dots \\ &= r'_1 A + \frac{t_1 r_2 t'_1 G^2 e^{j\delta t} A}{1 - r_1 r_2 G^2 e^{j\delta t}} = A \left(\frac{r_1 - r_2 G^2 e^{j\delta t}}{1 - r_1 r_2 G^2 e^{j\delta t}} \right). \end{aligned} \quad (1)$$

Based on Stokes relations given as $r = -r'$ and $tt' + r^2 = 1$, then the output power of the light can be calculated as

$$P_{out} = E_{out} \cdot E_{out}^* = A \cdot A^* \left| \frac{r_1 - r_2 G^2 e^{j\delta t}}{1 - r_1 r_2 G^2 e^{j\delta t}} \right|^2 = P_{in} \frac{(r_1 - r_2 G)^2 + 4r_1 r_2 G^2 \left(\sin\left(\frac{2\pi l \Delta \nu}{u}\right) \right)^2}{(1 - r_1 r_2 G)^2 + 4r_1 r_2 G^2 \left(\sin\left(\frac{2\pi l \Delta \nu}{u}\right) \right)^2}, \quad (2)$$

where $\Delta\nu$ is the frequency deviation from the central resonance frequency, which is calculated as $\Delta\nu = \nu - \nu_0$, l is the cavity length, and u is speed of light inside the gain medium, which is calculated as $u = c/n$. Based on Equation (2), given the reflectivity of the back facet of the cavity as $R_b = |r_2|^2 = 0.99$, the round-trip gain as $G = 2$, refractive index as $n = 3.5$, which is a typical value for InP, and the cavity length as $l = 600\mu\text{m}$, the gain spectra of the Fabry-Perot cavity as functions of reflectivity at the front facet, $R_f = |r_1|^2$, are plotted in Figure 5 (a).

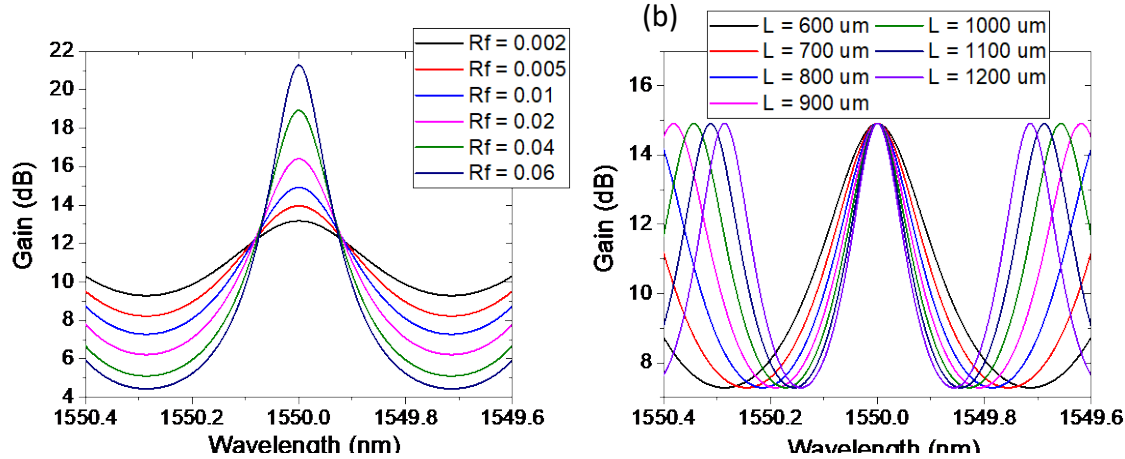


Figure 5 – Gain spectra of the Fabry-Perot cavity versus (a) reflectivity of the front facet, and (b) cavity length

It can be observed that the gain is increased, and the bandwidth is also narrowed with a larger front-facet reflectivity. However, it is worth noting that in the real situation, a gain increase will be limited by the gain saturation effects of the gain medium. Moreover, a large front-facet reflectivity results in less optical power to be injected inside the Fabry-Perot cavity, thus reducing the injection-locking efficiency. The narrowing of the gain bandwidth also results in higher sensitivity of the FP laser towards frequency offset and drifts. Figure 5 (b) plots the gain spectra of the FP laser under different cavity lengths, where the reflectivity at the front and back facets are $R_f = 0.01$ and $R_b = 0.99$ respectively, round-trip gain here is set as $G = 2$, and refractive index is $n = 3.5$. It can be observed that the free spectral range (FSR) between the adjacent oscillating wavelengths will be reduced with a longer cavity length. The increased density of the oscillating wavelengths means it becomes easier for the wavelength of the injected light to be matched with one mode for injection locking. However, with a fixed size of the gain area, longer cavity length will increase propagation loss thus reducing the output power of the FP-LD.

Except from the impacts of frequency detuning towards the injection ratio and SMSR, another important aspect is the required power to achieve injection locking given a certain SMSR. The sample FP laser exhibits one original longitudinal wavelength at around 1563.09 nm in our design. During the injection-locking process, small wavelength detunings are introduced for the master laser and, with reducing the wavelength detuning, four wavelengths are tested, including 1563.03 nm, 1563.05 nm, 1563.07 nm, and 1563.10 nm. The measured SMSR versus injected power under different wavelength tunings is shown in Figure 6. An interesting phenomenon is that although the maxima SMSR can be obtained with a smaller wavelength detuning, the operational injected power range is actually expanded with a lightly increased wavelength detuning. The reason behind this may be that under the injection-locking operation, the laser

cavity will be slightly heated up causing red-shifts of the gain peak for an intrinsic longitudinal mode. There is also a trade-off between the optimal SMSR and operation power range for injection locking.

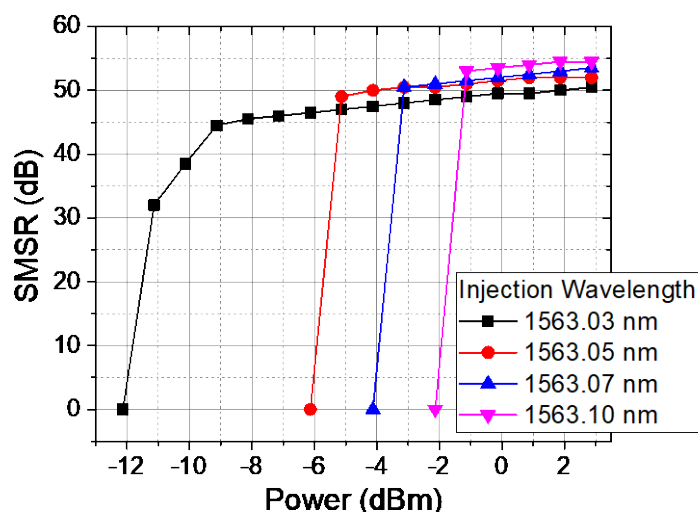


Figure 6 – SMSR versus injection power at different wavelengths

In our lab setup, the reflection-style coherent optical injection locking is used (Figure 3 (b)). Due to the requirement for a narrow frequency linewidth light source in a coherent system, a tunable ECL is selected as the master laser. The optical output power of the ECL is set to be 10 dBm. A FP-LD with 7-pin butterfly package, ~350μm cavity length, and a maximum output power up to +14 dBm is utilized as the slave laser. The ECL, with its wavelength tuned to match one of the longitudinal modes of the FP laser, injects light into the FP laser. Meanwhile, a DC bias is applied to the FP laser. The measured I-V curve (a) and output power at various bias voltage (b) of the FP laser are shown in Figure 7.

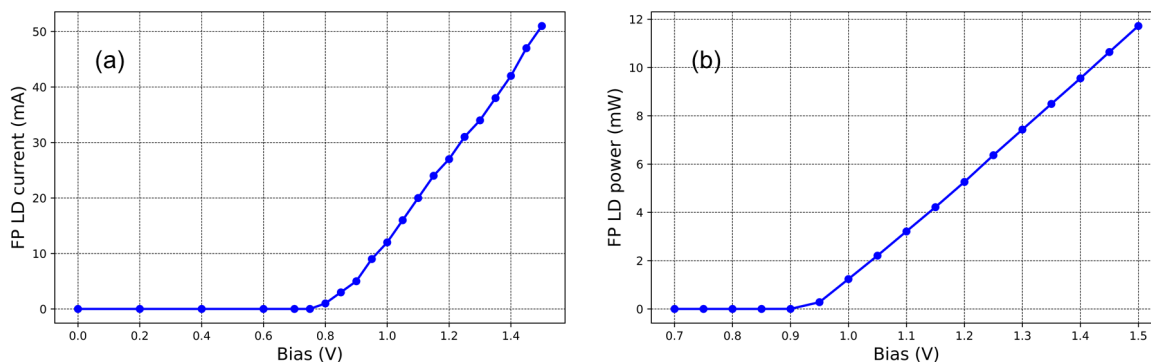


Figure 7 – FP laser I-V curve (a) and output power vs. bias (b)

By increasing the bias current gradually, one of the longitudinal modes of the FP laser is injection locked to the master ECL, while other modes are suppressed. As a result, single-mode operation of the FP laser is achieved at the selected wavelength. With its narrow spectral linewidth inherited from the ECL, this injection locked FP laser can be used as a coherent light source or local oscillator in the coherent system. Figure 8 shows the measured optical spectrum of the FP laser without external injection (a), and with ECL injection (b). The FP laser output power is set to be 5 dBm (1.11V bias, 20mA current). The center

wavelength of the ECL is set to be 1560.09 nm, which overlaps with one of the center cavity modes of the FP laser.

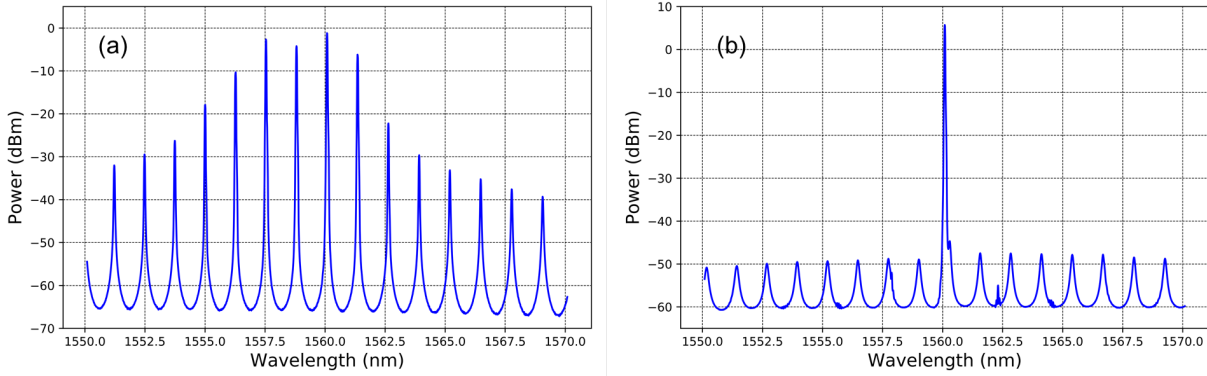


Figure 8 – Optical spectrum of the FP laser: (a) free running; (b) injection locked

The injection locking process, however, does not require a perfect overlap between the ECL and one of the FP laser modes. Under various injection conditions, when there's a frequency detuning between the ECL and the FP-LD modes, injection locking can still be achieved. It is important to understand the characteristics of the OIL laser frequency detuning, as it strongly affects the stability and reliability of the system. Theoretically, in the stable locking regime, operation of the OIL system can be described mathematically using a set of three differential equations [4-5]. The complex field of an injection-locked laser is very similar to that of a free running laser, with the addition of an injection term:

$$\frac{dE(t)}{dt} = \frac{1}{2}g\Delta N(1 + j\alpha)E(t) + kS_{inj} - j\Delta fE(t) \quad (3)$$

the slave laser's complex field $E(t)$ can be split into three differential equations that describe its photon number $S(t)$, phase $\phi(t)$, and carrier number $N(t)$. When under steady state operation, since there's no time variation in the slave laser's photon number, phase, and carrier number, the time derivative parts of the equations are equal to zero. Follow the solutions in [5], the steady state injection system can be described by the steady state phase ϕ_0 , steady state carrier number ΔN_0 , steady state photon number S_0 , and free-running photon number S_{fr} :

$$\phi_0 = \sin^{-1} \left\{ -\frac{\Delta\omega_{inj}}{k\sqrt{1+\alpha^2}} \sqrt{\frac{S_0}{S_{inj}}} \right\} - \tan^{-1}\alpha \quad (4)$$

$$\Delta N_0 = -\frac{2k}{g} \sqrt{\frac{S_{inj}}{S_0}} \cos\phi_0 \quad (5)$$

$$S_0 = \frac{S_{fr} - (\gamma_N/\gamma_P)\Delta N_0}{1 + (g\Delta N_0/\gamma_P)} \quad (6)$$

$$S_{fr} = \frac{J - \gamma_N N_{th}}{\gamma_P} \quad (7)$$

where g , k , N_{tr} , α , J , γ_N , and γ_P are the slave laser's linear gain coefficient, coupling rate, transparency carrier number, linewidth enhancement factor, current, carrier recombination rate, and photon decay rate, respectively. Under steady state, the phase value ϕ_0 falls into the range between $-\frac{\pi}{2}$ and $\cot^{-1}\alpha$ [4]. By choosing a ϕ_0 in the locking range, and rearrange (2) to determine the detuning frequency $\Delta f =$

$\Delta\omega_{inj}/2\pi = (\omega_{ML} - \omega_{fr})/2\pi$, which is the frequency difference between the master laser frequency ω_{ML} and the slave laser free-running frequency ω_{fr} . Also defining the field enhancement factor as $R_{FE} = \frac{A_0}{A_{fr}}$, which is the ratio between steady-state field magnitude and free-running field magnitude.

$$\eta_0 = \frac{c}{2n_g L} \frac{(1-R)}{\sqrt{R}} \sqrt{\frac{\eta_c P_{master}}{P_{slave}}} \quad (8)$$

where L is laser cavity length, n_g is group index ($n_g = 3.5$), R is reflectivity at the cleaved facet, η_c is the coupling efficiency of the laser ($\eta_c = 0.6$), and $\frac{P_{master}}{P_{slave}}$ is the external power injection ratio. These parameters are directly related to the laser physical design. The coupling rate k can be proportional to the injection ratio through: $k \sqrt{\frac{S_{inj}}{S_0}} = \frac{\eta_0}{R_{FE}}$. Here S_0 is the steady state photon number and S_{inj} is the injected photon number. With the above expressions, the slave laser's detuning frequency can be described as:

$$\Delta f = -\frac{k\sqrt{1+\alpha^2}}{2\pi} \sqrt{\frac{S_{inj}}{S_0}} \sin(\phi_0 + \tan^{-1}\alpha) = -\frac{\eta_0}{2\pi R_{FE}} \sqrt{1+\alpha^2} \sin(\phi_0 + \tan^{-1}\alpha) \quad (9)$$

One can see that the detuning frequency between master and slave lasers is directly related to the steady state phase and the external power injection ratio.

We experimentally measured the injection locking process under various injection ratio and detuning frequencies. In Figure 9 (a), the ECL frequency is adjusted to introduce the frequency detuning from one of the FP laser modes. The injection ratio is defined as the ratio between the master ECL output power and the slave FP-LD output power. The injection ratio is varied by adjusting the master ECL output power via a variable optical attenuator, while the slave FP laser power remains at +5 dBm unchanged. The blue dots in Figure 9 (a) indicate the injection locking process occurs under corresponding injection ratio and frequency detuning. It clearly shows that under higher injection ratio, the injection locking process is more forgiving to frequency detuning between the master and slave lasers. The results are in good agreement with the theoretical calculations reported in reference [4] and [5]. Optical spectrums of the slave FP laser under different locking conditions are shown in Figure 9 (b). The red curve indicates injection locked FP laser spectrum under low injection ratio with minimum frequency detuning, where the green curve is under high injection and negative frequency detuning. The blue curve is showing the condition with medium level injection ratio, when the frequency detuning is too large the slave FP laser is not injection locked and still operating in multi-mode. The corresponding data points of the three curves are labeled in Figure 9 (a) respectively. One can see that under strong optical injection, the side mode suppression ratio (the difference in optical power between the main mode and the largest side mode in decibels) of the injection locked FP laser is much higher compared with that under weak optical injection.

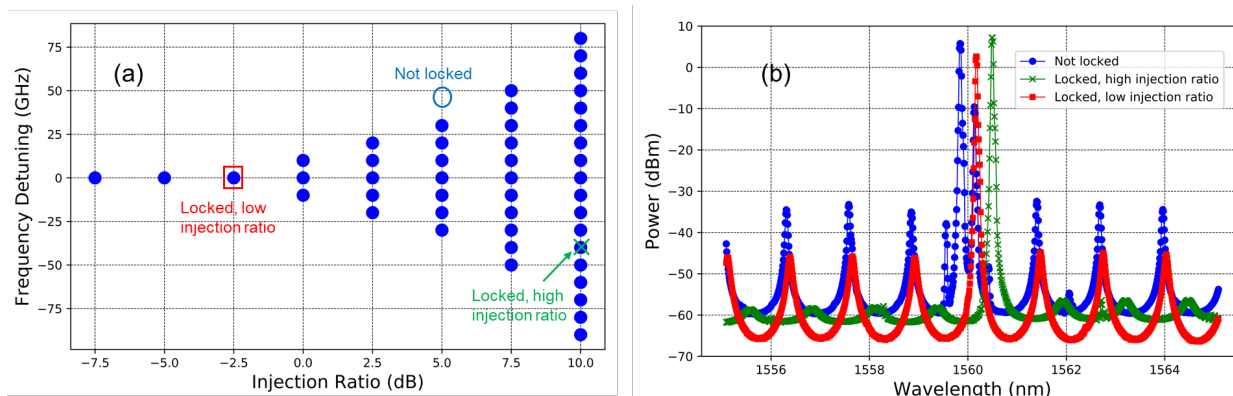


Figure 9 – Injection locking process study: (a) locking map under different injection ratio and frequency detuning; (b) optical spectrums of the slave FP laser under different locking conditions

Under 10 dB injection ratio, the SMSR of the injection locked FP laser under various frequency detuning is extracted, as shown in Figure 10. Under positive frequency detuning, the SMSR tends to decrease with increasing frequency detuning. Whereas under negative frequency detuning, the SMSR improves first with increasing detuning, then starts to decrease after the detuning reaches a certain level. This mainly attributes to the fact that the linewidth enhancement factor of the master laser introduces carrier variation which will induce shift of the slave FP laser gain towards longer wavelengths.

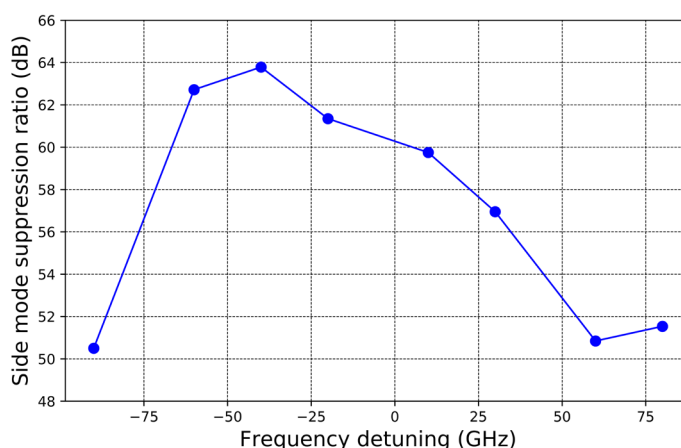


Figure 10 – Side mode suppression ratio under various frequency detuning

A key attribute of injection locking is that the detuning frequency range is asymmetrical with respect to the center frequency of the FP-LD side mode. If the master laser frequency is set at the center of the FP-LD side mode, it will achieve injection lock. However, if the master laser frequency is set slightly on the longer wavelength (lower frequency) side, it will have more tolerance to detuning. Therefore, it's more tolerant to maintain locking state in a larger frequency range compared with a "blue-shift" approach. This phenomenon is due to the linewidth enhancement factor of the master laser induced carrier variation which will induce the gain change of slave laser to longer wavelength.

5. Experimental Verifications

As the linewidth of the light source plays a critical role in the coherent optical communication systems, high resolution linewidth measurement were conducted on the injection locked FP laser and the comparison with a high quality ECL and a low-cost distributed feedback (DFB) laser was also performed. Due to limited resolution, grating-based optical spectrum analyzers (OSAs) are not suitable for this type of measurement. To achieve the desired resolution for characterizing our laser linewidth, the delayed self-heterodyne measurement technique was adopted here.

The laser linewidth measurement setup is shown in Figure 11. The output light from the laser under test is first split into two paths by a 3-dB fiber optic coupler. One path is sent through a Mach-Zehnder interferometer (MZI) driven with 2.5 GHz. The MZI shifts the detection frequency away from 0 Hz in the RF spectrum analyzer. Another path is sent through a delay line of 5-km SMF-28 fiber with a polarization controller. As a result, the laser light from the two paths are uncorrelated after the long delay. Both paths are then superimposed on another 3-dB fiber optical coupler while the resulting beat note centered at 2.5GHz is recorded with an avalanche photodiode (APD), and the RF spectrum is shown on the RF spectrum analyzer. With the interference between the two optical paths, the photocurrent generated in the APD includes both the direct intensity detection and the heterodyne frequency mixing term. As a result, the optical spectrum of the laser auto correlates with the delayed version of itself, in the frequency domain the detected autocorrelation function has a 3dB linewidth twice of the original laser 3dB linewidth.

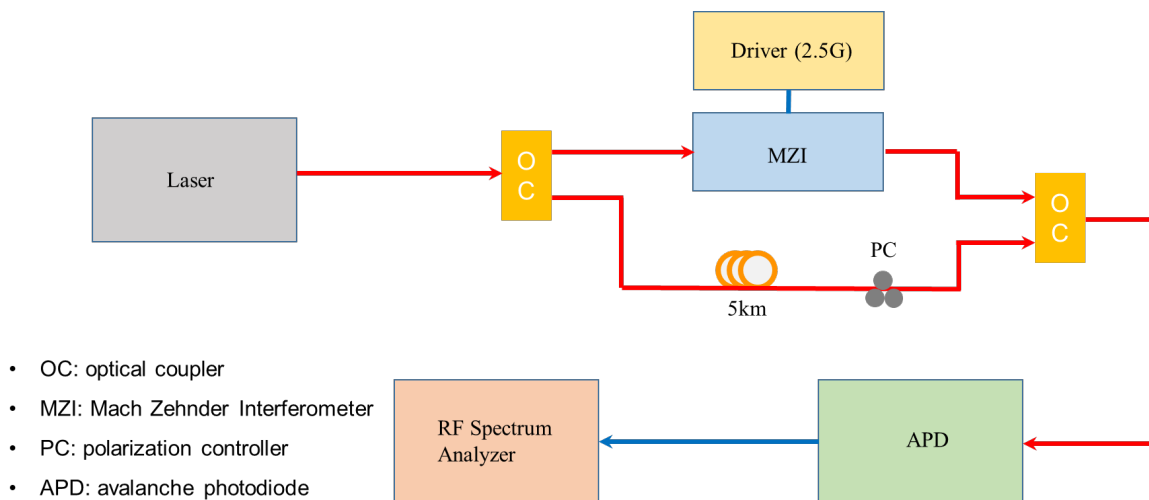


Figure 11 – Delayed self-heterodyne laser linewidth measurement setup

Based on the delayed self-heterodyne method, the measured linewidth results are shown in Figure 12. The ECL linewidth is within the manufacturer's specifications, and the injection-locked FP laser shows similar performance. Both the ECL and the injection-locked FP-LD have linewidth under 50kHz, which ensures good performance in a coherent system.

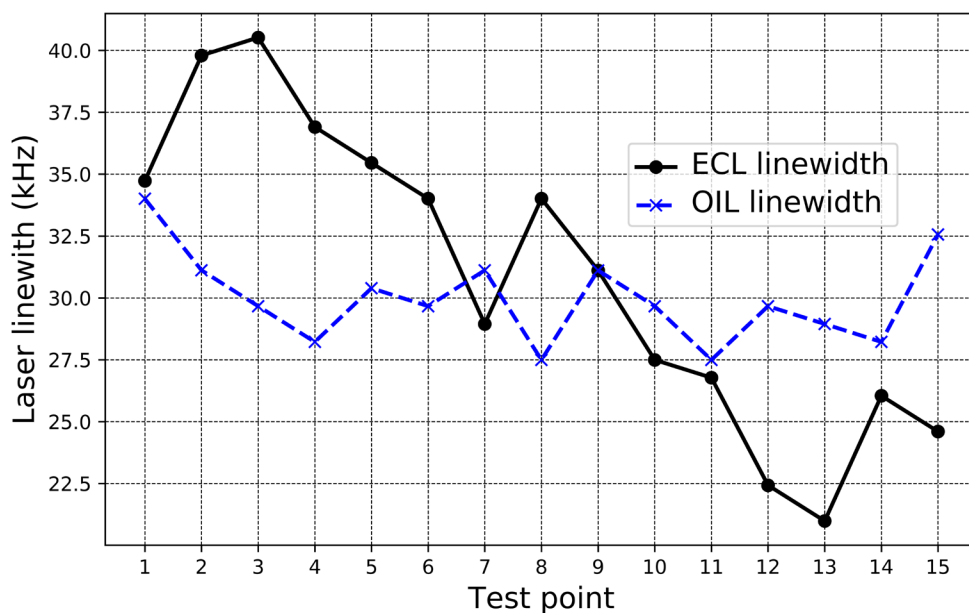


Figure 12 – Measured ECL and injection-locked FP-LD linewidth

As a reference, we also measured the linewidth of a DFB laser, with the results are shown in Figure 13. The DFB laser is also a single-frequency laser, and the cost is relatively low compared with the ECL. However, the linewidth of the DFB laser is also much wider compared with either the ECL or the injection-locked FP-LD, in the range of a few MHz.

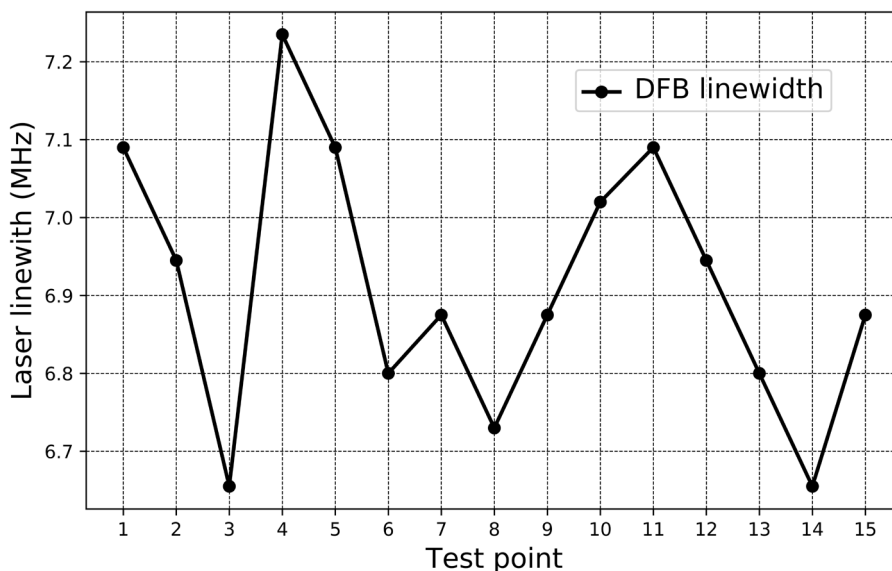


Figure 13 – Measured low-cost DFB laser linewidth

The transmission performance of the coherent optical system with injection-locked FP-LD as the laser source has also been experimentally verified. The system diagram of the coherent optical link is shown in Figure 14.

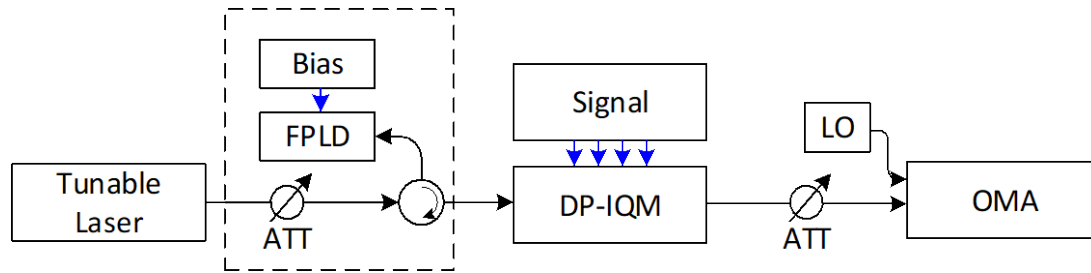


Figure 14 – System diagram for BER measurement

The light from a tunable ECL is attenuated and fed into an FP laser for injection locking. The wavelength of the laser is carefully tuned to be around 1561.3 nm, which is matched with one longitudinal mode of the FP laser. A bias controller is used to control the output power of the FP laser to be around 10 dBm. Then light from the FP laser enters into a dual-polarization IQ modulator where the electrical signals are converted from the electrical to optical domain. A coherent optical modulation analyzer (OMA) is used to receive and sample the signals before offline digital signal processing is used for signal recovery. An optical attenuator is also used here to adjust the received power of OMA. In the experiments, three kinds of data modulation formats are applied, including 32-GBaud dual-polarization quadrature-phase-shift keying (DP-QPSK), 60.375-GBaud dual-polarization 16-ary quadrature-amplitude modulation (DP-16QAM), and 40-GBaud dual-polarization 64-ary quadrature-amplitude modulation (DP-64QAM), which correspond with total data bit rates of 128 Gbit/s, 483 Gbit/s, and 480 Gbit/s, respectively. The measured bit-error rates versus received optical power with injection locking and without it in the ECL case are shown in Figure 15 (a) to (c) in regards of DP-QPSK, DP-16QAM, and DP-64QAM, respectively. It can be observed that the power penalties brought by coherent injection-locking is insignificant for DP-QPSK and DP-16QAM, where the average power penalties are less than 0.3 dB. However, for the 40-GBaud DP-64QAM, the power penalty is slightly increased.

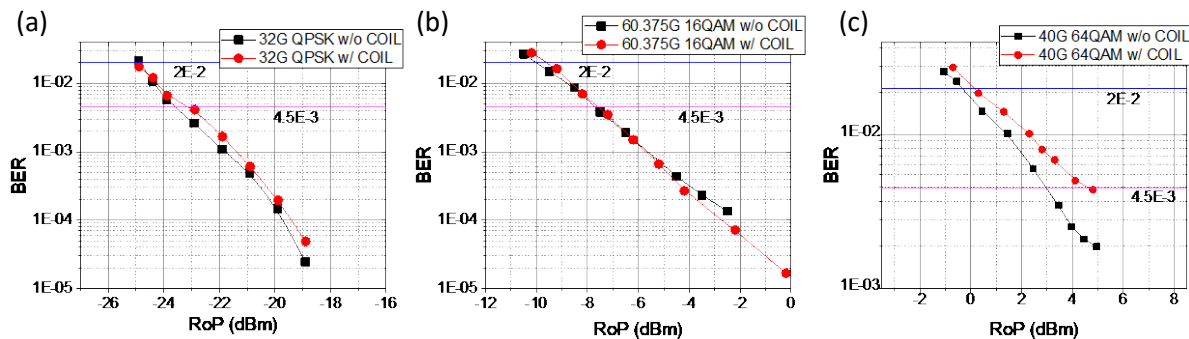


Figure 15 – BER performance with and without applying COIL for (a) 32-Gbaud DP-QPSK, (b) 60.375-GBaud DP-16QAM, and (c) 40-GBaud DP-64QAM

6. Applications and Cost Analysis

The generation of a high spectral purity optical signal with an FP laser has been thoroughly demonstrated in earlier sections. The question remains how this approach can be leveraged to implement low cost coherent systems. The coherent system still needs a source that is spectrally pure which has higher cost. The answer lies in sharing the cost of the higher performance master laser signal. How the master laser is shared has implications in the cost and in the type of applications where this approach can be used. In the access environment, it is common to have hubs with serving areas covering 30,000 to 50,000 households. In a 500 homes passed per node architecture this results in 60 to 100 nodes per hub. In the downstream direction, there are typically dedicated fibers extending to the fiber nodes from a central hub location. It is therefore possible to share a master laser signal by distributing it among the many fiber nodes. Figure 6 shows how you can use a signal reaching the FP at -10 dBm and still injection lock it. Therefore if the master laser is transmitting at +10 dBm optical power, the 20 dB budget can be used to split the signal 64 ways in the hub sending it fiber nodes and remote destinations served from the hub and still have enough power budget for 40 km fiber links. A hub with one or two master lasers can remotely injection locked FP lasers at fiber nodes, base-station and businesses served from the hub (Figure 16).

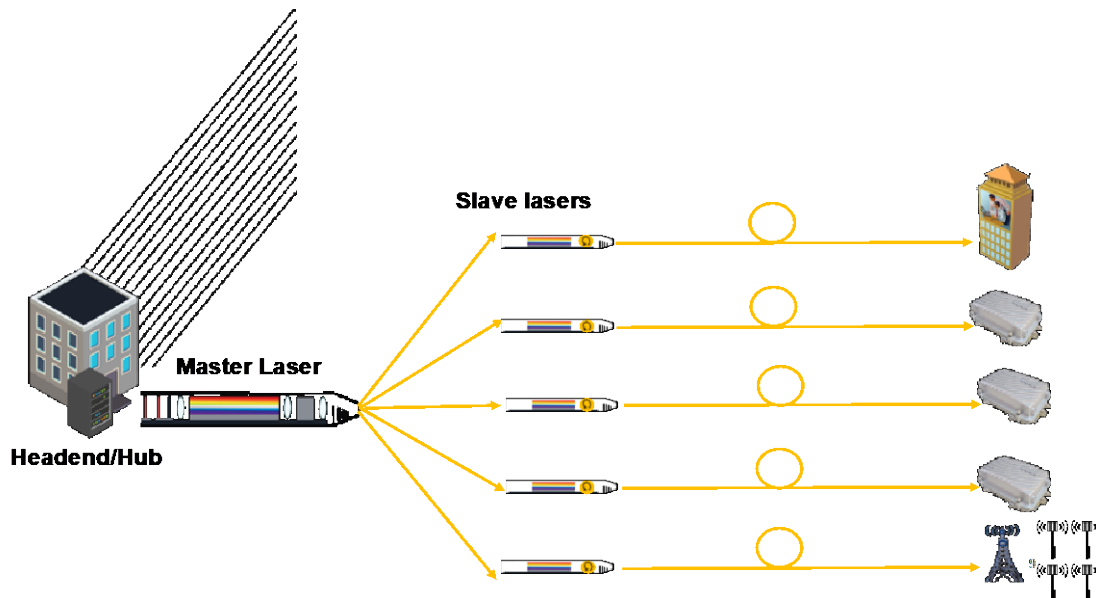


Figure 16 – Application I: Multiple fibers to different destinations

Since the cost of the FP laser is about two orders of magnitude lower than the cost of an ECL, this use case leads to a significant cost reduction of P2P coherent optics links. The cost of the coherent laser could easily drop by a factor of 40. The split ratio of 64 was assumed using commercially available FP lasers. With optimization of the laser parameters such as the cavity length, facet reflectivities can further improve the injection locking effectiveness. A future derivative of this application could be the support of point-to-multipoint scenarios.

So far we have been describing the use of a single master laser with single frequency emission that is split towards multiple destinations. Recent technological advancement have been in developing comb lasers [7-8]. Comb lasers can generate multiple high-fidelity optical signals that are equally spaced in wavelength or frequency. The comb laser can be used to injection locked multiple FP lasers, each using a different tone generated by the comb laser. This in turn can be used to populate a single fiber with DWDM channels (Figure 17).

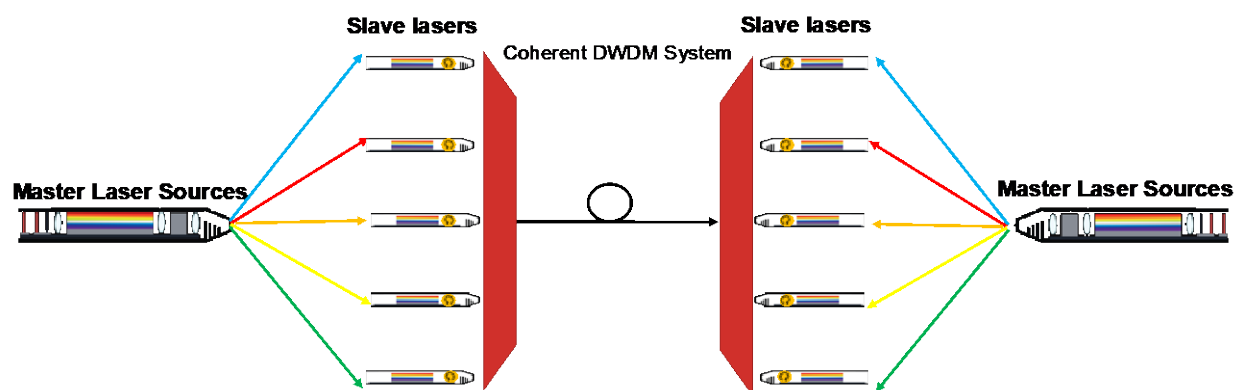


Figure 17 – Application II: Comb source for DWDM systems over single fiber

Using comb lasers with tones separated 100 GHz or 50 GHz apart could respectively generate 40 or 80 DWDM coherent signals in the C-band. Injection locking becomes a strategic tool for cost reduction when the network architecture lends itself to multiple destinations or multiple wavelengths. The high receive sensitivity of coherent optics also allows this sharing to be done remotely so that the cost of remote devices is reduced.

Wavelengths utilized are determined at the hub central location. Since the slave devices just lock to the master laser wavelength, the slave FP laser is not wavelength specific meaning only one part is needed in a remote location regarding which wavelength is to be used.

Systems leveraging optical amplification could achieve some of the functionality described here however cost and simplicity of a Fabry-Perot laser is most attractive.

Conclusions

Coherent optics technology offers a future-proof solution for cable operators to meet bandwidth demand without the need for retrenching new reinforcement fibers. Cost reduction of coherent laser source is of great interest when bringing coherent optics into access applications. In this paper, a disruptive low-cost injection-locked FP Laser source has been proposed for coherent access networks. Through injection locking, the slave laser closely adopts the optical frequency and linewidth characteristics of the master laser which can be shared between multiple child lasers. As a result, the cost of the coherent optical transceiver can be significantly reduced. This paper introduces the operation principle of FP-LD injection locking as well as design theory. The detuning condition and linewidth characterization have been experimentally carried out with FP-LD samples. The comparison of transmission performance for different laser source is also presented experimentally. This paper also shows the promising applications of the injection locked FP-LD and the frequency comb in coherent access system.

Abbreviations

| | |
|------|-----------------------------------------|
| APD | avalanche photodiode |
| BER | bit error rate |
| CD | chromatic dispersion |
| CMOS | complementary metal–oxide–semiconductor |
| CW | continuous-wave |

| | |
|--------|--------------------------------------------------|
| DAA | distributed access architecture |
| DFB | distributed feedback (laser) |
| DOCSIS | Data-over-Cable Service Interface Specifications |
| DP | Dual polarization |
| DSP | digital signal processing |
| DWDM | dense wavelength division multiplexing |
| ECL | external cavity laser |
| FP-LD | Fabry-Perot Laser Diode |
| FSR | free spectral range |
| GHz | gigahertz |
| HFC | hybrid fiber-coax |
| ISBE | International Society of Broadband Experts |
| km | kilometer |
| LO | local oscillator |
| MGM | mirror-gain medium-mirror |
| MHz | megahertz |
| MZI | Mach-Zehnder interferometer |
| MZM | Mach-Zehnder modulator |
| ODC | Optical Distribution Center |
| OIL | optical injection locking |
| OLT | optical line terminal |
| OMA | optical modulation analyzer |
| P2P | Point-to-Point |
| PMD | polarization mode dispersion |
| PON | passive optical network |
| QAM | quadrature amplitude modulation |
| QPSK | quadrature phase shift keying |
| RF | radio frequency |
| SMF | single mode fiber |
| SMSR | side mode suppression ratio |
| SNR | signal to noise ratio |
| SCTE | Society of Cable Telecommunications Engineers |

Bibliography & References

- [1] Cable Television Laboratories, Inc. “P2P Coherent Optics Physical Layer 1.0 Specification”, June 29, 2018. <https://specification-search.cablelabs.com/P2PCO-SP-PHYv1.0>
- [2] Cable Television Laboratories, Inc. “P2P Coherent Optics Physical Layer 2.0 Specification”, March 11, 2019. <https://specification-search.cablelabs.com/P2PCO-SP-PHYV2.0>
- [3] Z. Jia, L. A. Campos, C. Stengrim, J. Wang, C. Knittle, “Digital Coherent Transmission for Next-Generation Cable Operators’ Optical Access Networks,” Oct. SCTE/ISBE Cable-Tec Expo’17, 2017.
- [4] Q. T. Nguyen, P. Besnard, L. Bramerie, A. Shen, A. Garreau, et al., “Using optical injection of Fabry-Perot lasers for high-speed access in optical telecommunications”, SPIE Photonics Europe 2010, Bruxelles, Belgium. SPIE (ISBN 9780819481931), 7720, pp.77202D, (2010).
- [5] E. K. Lau, H. Sung and M. C. Wu, “Frequency Response Enhancement of Optical Injection-Locked Lasers,” in IEEE Journal of Quantum Electronics, vol. 44, no. 1, pp. 90-99, Jan. 2008.

- [6] E. K. Lau, L. J. Wong and M. C. Wu, "*Enhanced Modulation Characteristics of Optical Injection-Locked Lasers: A Tutorial*," in IEEE Journal of Selected Topics in Quantum Electronics, vol. 15, no. 3, pp. 618-633, May-June 2009.
- [7] M. D. G. Pascual, V. Vujicic, J. Braddell, F. Smyth, P. Anandarajah and L. Barry, "Photonic Integrated Gain Switched Optical Frequency Comb for Spectrally Efficient Optical Transmission Systems," in IEEE Photonics Journal, vol. 9, no. 3, pp. 1-8, June 2017.
- [8] V. Torres-Company et al., "Laser Frequency Combs for Coherent Optical Communications," in Journal of Lightwave Technology, vol. 37, no. 7, pp. 1663-1670, 1 April, 2019.